GaAs Nanowire pn-Junctions Produced by Low-Cost and High-Throughput Aerotaxy

Barrigón, E.; Hultin, O.; Lindgren, D.; Yadegari, F.; Magnusson, M. H.; Samuelson, L.; Johansson, L. I.M.; Björk, M. T.

Published in:
Nano Letters

DOI:
10.1021/acs.nanolett.7b04609

2018

Document Version:
Publisher's PDF, also known as Version of record

NANO LETTERS

Letter

Cite This: Nano Lett. 2018, 18, 1088−1092

pubs.acs.org/NanoLett

GaAs Nanowire pn-Junctions Produced by Low-Cost and High-Throughput Aerotaxy

E. Barrigón,[§,†,‡] O. Hultin,[§,‡] D. Lindgren,[§,†] F. Yadegari,[†] M. H. Magnusson,[‡] L. Samuelson,[†,‡] L. I. M. Johansson,[*,†] and M. T. Björk[†]

[†]Sol Voltaics AB, Scheelevägen 63, 223 63 Lund, Sweden

[‡]NanoLund and Division of Solid State Physics, Lund University, Box 118, 221 00 Lund, Sweden

Supporting Information

ABSTRACT: Semiconductor nanowires could significantly boost the functionality and performance of future electronics, light-emitting diodes, and solar cells. However, realizing this potential requires growth methods that enable high-throughput and low-cost production of nanowires with controlled doping. Aerotaxy is an aerosol-based method with extremely high growth rate that does not require a growth substrate, allowing mass-production of high-quality nanowires at a low cost. So far, pn-junctions, a crucial element of solar cells and light-emitting diodes, have not been realized by Aerotaxy growth. Here we report a further development of the Aerotaxy method and demonstrate the growth of GaAs nanowire pn-junctions. Our Aerotaxy system uses an aerosol generator for producing the catalytic seed particles, together with a growth reactor with multiple consecutive chambers for growth of material with different dopants. We show that the produced nanowire pn-junctions have excellent diode characteristics with a rectification ratio of >10^5, an ideality factor around 2, and very promising photoresponse. Using electron beam induced current and hyperspectral cathodoluminescence, we determined the location of the pn-junction and show that the grown nanowires have high doping levels, as well as electrical properties and diffusion lengths comparable to nanowires grown using metal organic vapor phase epitaxy. Our findings demonstrate that high-quality GaAs nanowire pn-junctions can be produced using a low-cost technique suitable for mass-production, paving the way for industrial-scale production of nanowire-based solar cells.

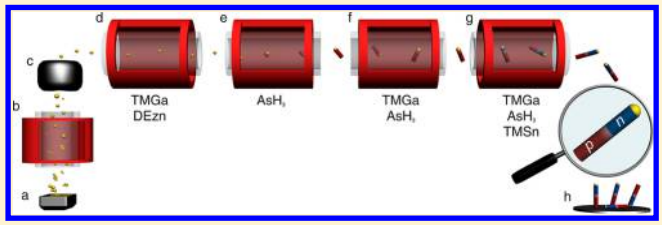

KEYWORDS: *Aerotaxy, nanowires, pn-junction, GaAs, electron beam induced current, hyperspectral cathodoluminescence*

Semiconductor nanowires are expected to be important building blocks for future electronics, light-emitting diodes (LEDs), and solar cells.[1−3] The resonant light absorption properties of nanowires give rise to light collection from an area much larger than their cross section;[4,5] a periodic nanowire array thus produces a photogenerated current equivalent to that of a planar semiconductor structure while using significantly less material. This approach has been realized successfully by several groups[6−14] with reported photovoltaic power conversion efficiencies as high as 17.8% for etched nanowires[8] and 15.3% for grown nanowires,[6] the latter with a surface area coverage of only 13%. However, producing large quantities of high-quality III−V semiconductor nanowires with conventional methods (e.g., molecular beam epitaxy or metal−organic vapor phase epitaxy) seems unfeasible, given the low throughput and high cost of these batch-based and slow epitaxial growth processes, together with the need of expensive monocrystalline substrates. It is thus important to identify and develop alternative methods to reduce production costs, especially for large-area applications such as solar cells.

Heurlin et al. addressed the cost limitations of conventional techniques by growing GaAs nanowires in an ultrafast and substrate-less Aerotaxy process.[15] This technique allows for continuous production of high-quality nanowires in the aerosol phase with very high growth rates of up to 1 μm/s, which is 20 to 1000 times higher than in traditional substrate based batch processes.[15,16] It has also been demonstrated that Aerotaxy can be used for manufacturing ternary materials with a tunable band gap.[17] However, to realize production of nanowire-based devices such as LEDs and solar cells using this technique, a crucial prerequisite is growth of high-quality pn-junctions, which has not been demonstrated up until now.

Here we address this need, report further development of the Aerotaxy method, and demonstrate its versatility by producing GaAs nanowires with pn-junctions intended for solar cell applications. The method builds on previous work[15] by adding additional growth stages to the reactor. Electrical measurements, electron-beam induced current (EBIC), and hyperspectral cathodoluminescence (CL) revealed good diode characteristics and photoresponse, a well-defined pn-junction and high doping levels of the p- and n-sections of the produced nanowires. Our results show that it is possible to produce high-quality nanowire pn-junctions with a low-cost and high-

Received: October 30, 2017
Revised: December 29, 2017
Published: December 30, 2017

DOI: 10.1021/acs.nanolett.7b04609
Nano Lett. 2018, 18, 1088−1092

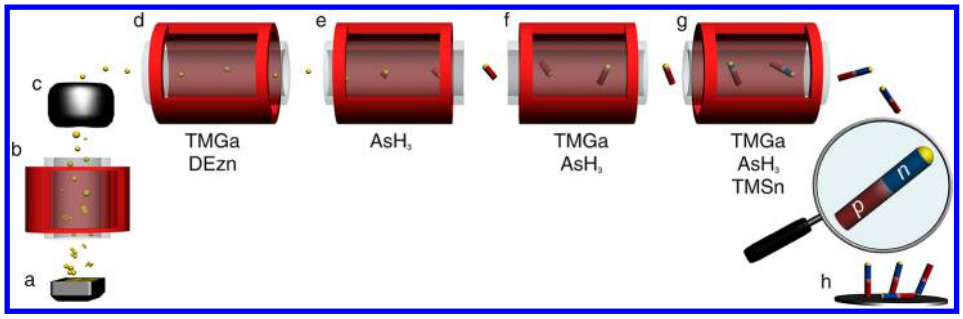

Figure 1. Aerotaxy growth of nanowire pn-junctions. (a) Au aerosol generation; (b) sinter furnace for Au compaction; (c) DMA for Au particle size selection; (d) alloying chamber; (e) p-segment growth; (f) growth under nominally intrinsic conditions; (g) n-segment growth; (h) nanowire deposition.

throughput technique, a big step toward industrial-scale production of large area nanowire-based solar cells. In contrast to nanowires grown from a substrate, Aerotaxy nanowires are produced in a disordered state. In order to fabricate large area solar cells, it is necessary to align the nanowires vertically with the right polarity in an array. In the Supporting Information, we show that this is possible by using an ink and demonstrate it for a 30 mm × 30 mm membrane.

In order to produce GaAs nanowires with a pn-junction, we used an Aerotaxy growth system with Au nanoparticles as catalytic seeds in a reactor with different dopants in consecutive growth chambers. We first describe the setup and operating principles of the Aerotaxy system employed and then present an evaluation of the electrical and optical properties of the nanowires produced.

The Aerotaxy system (Figure 1) is designed and built by Sol Voltaics and consists of two main parts: (i) an aerosol system based on conventional techniques for producing the catalytic seed particles, and (ii) an Aerotaxy growth reactor. The aerosol system contains an arc reactor for evaporation of seed particle material (Figure 1a), a tube furnace for particle compaction (Figure 1b), and a differential mobility analyzer (DMA) for nanoparticle size selection (Figure 1c).[18] Because the tool capacity is determined by the flow rate and particle density, a high-density aerosol is important for high-volume production. A seed particle concentration of 2×10^6 #/cm^3 with a diameter of 120 nm was used. The Aerotaxy reactor consists of an alloying chamber, followed by three growth chambers. Each growth chamber has a tunable temperature and its own precursor injection for using different materials. In the alloying chamber (Figure 1d), trimethylgallium (TMGa) is introduced together with diethylzinc (DEZn) to form an alloy with the seed particle. In the first growth chamber (Figure 1e), a crystal precipitates from the seed particle, forming the first part of the p-segment of the nanowire. Only arsine (AsH_3) is injected whereas Ga and Zn is supplied from the alloyed seed particle. In the second growth chamber (Figure 1f), the nanowire growth is continued by injection of TMGa and AsH_3, further depleting the seed particle of Zn. In the last chamber (Figure 1g), the n-segment is grown by injection of tetramethyltin (TMSn) along with TMGa and AsH_3. The growth temperature was 500 °C with an alloying temperature of 410 °C and the growth time of the nanowires was approximately 9 s. In the last step, the nanowires are collected using an electrostatic precipitator (ESP) and deposited on a Si substrate (Figure 1h). Note that the nanowires could be deposited onto any kind of substrate, into a filter, or a solution.

Scanning electron microscopy (SEM) images of the produced catalytic seed particles and the resulting nanowires deposited on a carrier substrate are displayed in Figure 2a,b,

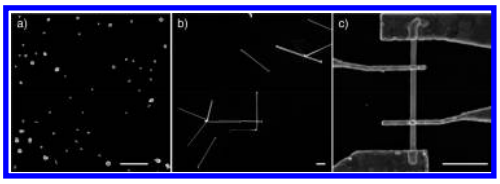

Figure 2. (a) Typical Au nanoparticles produced in the Aerotaxy system; (b) Aerotaxy nanowires with pn-junction; (c) a nanowire (device 3) contacted for characterization. The scale bar in each image corresponds to 1 μm.

respectively. The dimensions of 25 randomly selected nanowires were measured from SEM images. The average nanowire length was 4.6 μm (σ = 15%) and the average diameter was 120 nm (σ = 14%). No tapering could be observed from the SEM images, indicating that any parasitic shell growth is minimal (<10 nm).

To assess the electrical and optical properties of the produced pn-junction nanowires, a few selected nanowires were characterized with dark and light intensity-dependent current−voltage ($I-V$), EBIC, and hyperspectral CL measurements, all performed at room temperature. Prior to characterization, the nanowires were transferred to a Si substrate insulated with 100 nm SiO_2 and 10 nm HfO_2. Thereafter, several nanowire devices were fabricated with four metal contacts: two contacts on the p-side and two on the n-side (Figure 2c). This geometry was chosen to enable $I-V$ characterization with limited influence of the contact properties. The contacts were defined to the nanowires in PMMA950A6 resist using electron beam lithography (Raith 150). Ti/Au (10/150 nm) was deposited using thermal evaporation and resist lift-off was done in acetone.

The $I-V$ measurements were performed in a Cascade probe station connected to a Keithley 4200 SCS. In dark conditions, a diode characteristics with ideality factors between 1.9 and 2.0 and rectification of more than 10^5 at ±1 V were observed (Figure 3a). To evaluate the photovoltaic properties, the current−voltage behavior of device 1 from Figure 3a was examined at different illumination intensities (Figure 3b). The device was illuminated by a 532 nm diode laser and the light intensity controlled by a set of neutral density filters. The plotted relative intensity is normalized with respect to the greatest illumination intensity (approximately 400 mW/cm^2). When illuminated with the greatest intensity (i.e., relative

DOI: 10.1021/acs.nanolett.7b04609
Nano Lett. 2018, 18, 1088−1092

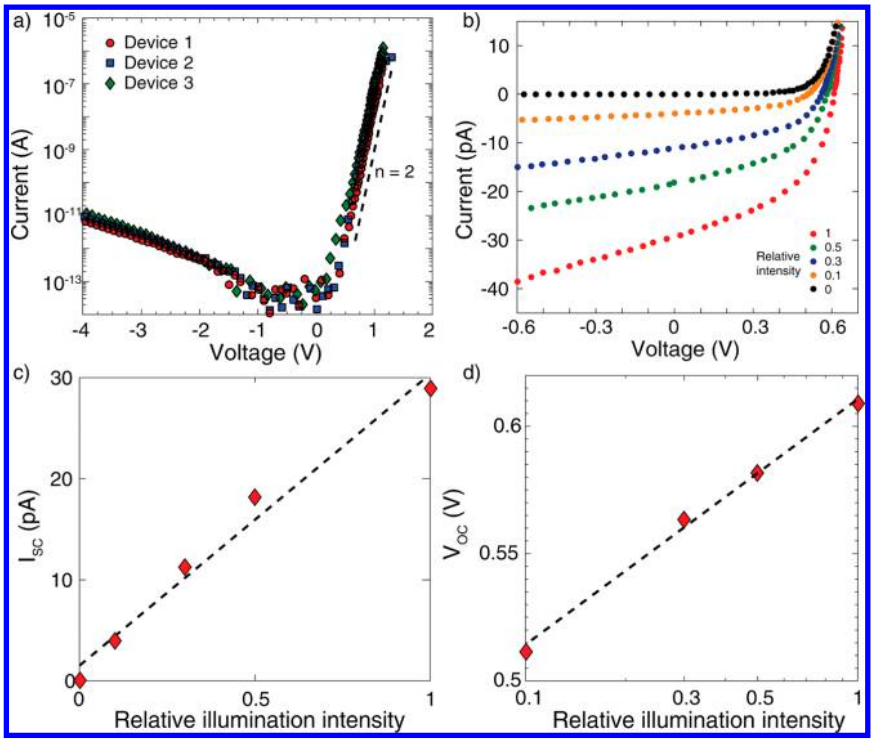

Figure 3. Electrical characteristics under dark and illuminated conditions. (a) Dark current−voltage characteristics for three illustrative nanowire devices. The devices show similar characteristics with ideality factors around 2. (b) Current−voltage characteristics of device 1 under laser illumination of different intensities. The relative intensity is normalized with respect to the maximum intensity of the laser. (c) Short-circuit current as a function of relative illumination intensity, derived from the measurement in (b). (d) Open-circuit voltage as a function of relative illumination intensity, derived from the measurement in (b). The dashed lines in (c,d) are intended as guides to the eye.

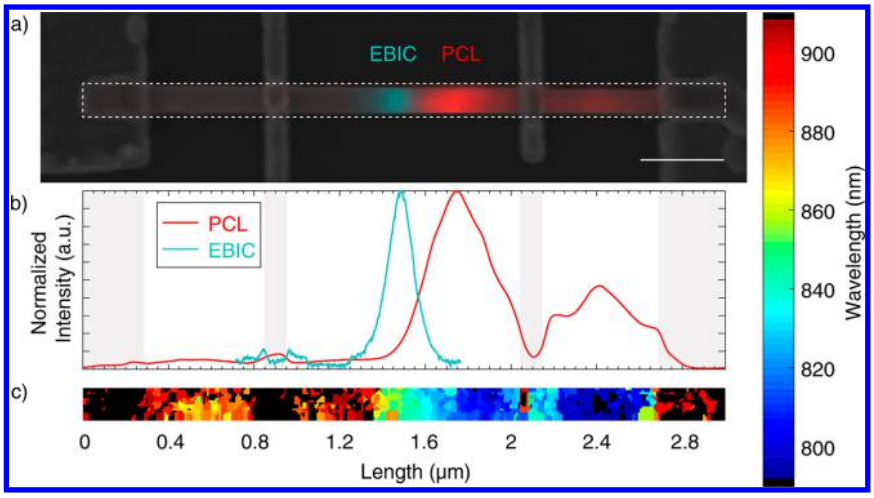

Figure 4. (a) Composite image of the EBIC (cyan) and PCL signal (red) overlaid over a SEM micrograph of the nanowire device (gray and outlined). The scalebar corresponds to 400 nm. (b) Corresponding and normalized EBIC (cyan) and PCL (red) intensity profiles along the nanowire. The four contacts seen in (a) are also indicated with gray blocks. (c) Corresponding peak wavelength map of the region indicated by a dashed rectangle in (a) for the range 790−910 nm; blue and red pixels indicate a peak position blueshift (n-type) or redshift (p-type) relative to intrinsic GaAs; black pixels fall outside the range as specified with the color bar on the right-hand side.

intensity = 1), the device showed a short circuit current I_{SC} of 29 pA (220 mA/cm^2 normalized to the nanowire cross-section area), an open circuit voltage V_{OC} of 0.61 V and a fill factor of 48%. As expected, the I_{SC} increased linearly with illumination intensity (Figure 3c) and the V_{OC} increased linearly with the logarithm of the illumination intensity (Figure 3d). The relatively low V_{OC} values are expected for unpassivated GaAs nanowire photovoltaics and can be attributed to the high surface recombination velocity of GaAs.[19,20] Surface passivation is expected to increase the V_{OC} significantly and to improve the ideality factor. The I−V curves measured under illumination show signs of a shunt resistance, possibly due to the surface states or to lateral overgrowth of n-type material forming a very thin shell over the p-region[1]. Further studies are needed to conclusively determine the cause of the shunt resistance. The electrical characteristics clearly demonstrate the existence of a pn-junction in the nanowire and that it functions as a single nanowire photovoltaic cell with promising performance.

DOI: 10.1021/acs.nanolett.7b04609
Nano Lett. 2018, 18, 1088−1092

In order to spatially identify the location of the pn-junction and to study the doping concentration in the nanowires, EBIC and hyperspectral CL measurements were performed on the devices from Figure 3a in a Hitachi SU8010 SEM. The acceleration voltage was set to 5 kV, which ensured an optimal excitation volume within the nanowires, and the probe current to approximately 50 pA, which was sufficient to acquire a signal from all locations of the exposed nanowire. For the EBIC measurements, the metal contacts of the devices were contacted with micromanipulators and performed at zero bias using a Kleindiek probestation system. The CL measurements were performed under open-circuit conditions using a Delmic Sparc system, using a spectral resolution of approximately 15 nm. A superposition of the EBIC current measured along the axial direction of a wire with a panchromatic CL (PCL) and a SEM image of device 3 is shown in Figure 4a, while the corresponding EBIC and PCL intensity profiles are shown in Figure 4b. Additional EBIC data can be found in the Supporting Information. The position of the peak of the Gaussian-like EBIC profile indicates that the pn-junction was located near the middle of the wire. The decreasing tails of the profile could be fitted to single exponential curves, which revealed effective minority carrier diffusion lengths of around 70 nm for both electrons in the p-segment and holes in the n-segment. The estimated values are in good agreement with values reported in literature for unpassivated nanowires of similar diameter, grown by metal organic vapor phase epitaxy (MOVPE),[21] which indicates that the Aerotaxy process can produce nanowires with at least similar quality to MOVPE.

The PCL image in Figure 4a, which represents the integrated intensity over the range from 770 to 1030 nm of the area (indicated with a dashed rectangle) reveals that the dominating luminescence originates from the n-doped (right-hand) side of the nanowire. In contrast, the intensity remains low on the p-doped (left-hand) side. The intensity change is expected in GaAs depending on the doping type.[22] The map in Figure 4c displays the peak position wavelength at each pixel, which allows us to identify the doping type and the location of the pn-junction. On the p-doped side, the peak position was found to be redshifted compared to intrinsic GaAs, which is characteristic for p-type GaAs, whereas on the n-doped side, the peak position was blueshifted, characteristic for n-type GaAs.[22] The estimated hole concentration for the p-doped side was approximately 1×10^{19} cm^{-3}.[22] In the n-segment, the peak position was found to be blueshifted from the region of the EBIC signal to the outer contact, indicating an increase in the effective electron concentration. Close to the outer contact/exposed nanowire interface, the concentration was estimated to be approximately 2×10^{19} cm^{-3}. The observation is in agreement with the intensity decrease toward the outer contact as it is known that nonradiative recombination processes starts to dominate above a certain doping concentration.[22] Note that the spatial resolution was limited by the effective diffusion length of around 70 nm.

Finally, Figure 4 also shows that there is a good agreement between EBIC and CL performed on the same nanowire. The EBIC maximum coincides with a clear shift in CL peak position and with the onset of the increase in CL intensity. The results from the EBIC and CL measurements show that there is a pn-junction located in the middle of the nanowire and that the p- and n-segments are highly doped.

Because of the high p-doping level, even if a very thin (<10 nm) parasitic n-type shell is present around the p-region, our calculations show that the shell will be depleted and only have minor effect on the devices, not affecting the conclusions of this study.

In summary, we have demonstrated that nanowire-based devices with axial GaAs pn-junctions can be produced by a continuous, high-throughput and substrate-less Aerotaxy growth process. The fabrication of semiconductor nanowires was realized by using consecutive, in-line reactors to grow different segments of the nanowires. The resulting nanowires exhibited a well-defined pn-junction, high doping levels with electrical properties and diffusion lengths comparable to nanowires grown by MOVPE. Compared to MOVPE, the production costs of the Aerotaxy approach are dramatically reduced, enabling solar cell production at significantly lower costs.

We anticipate that including additional reactors to the Aerotaxy system may largely expand the range of possible device designs using Aerotaxy. In particular, the growth of more complex structures, such as shell growth for passivation, or of heterostructures could become possible. Aerotaxy is a versatile growth process with possibilities that we are only beginning to explore with the potential to play a very important role for next generations of optoelectronics.

■ ASSOCIATED CONTENT

Supporting Information

The Supporting Information is available free of charge on the ACS Publications website at DOI: 10.1021/acs.nanolett.7b04609.

Alignment of Aerotaxy nanowires into an ordered array. Additional EBIC measurements (PDF)

■ AUTHOR INFORMATION

Corresponding Author

*E-mail: linda.johansson@solvoltaics.com.

ORCID

O. Hultin: 0000-0002-7142-4666

Author Contributions

[§]These authors contributed equally to this work

Notes

The authors declare the following competing financial interest(s): E. Barrigon: Part-time employee of Sol Voltaics AB. O. Hultin: No competing interests. D. Lindgren: Employee of Sol Voltaics AB. F. Yadegari, L.I.M. Johansson: Employees of Sol Voltaics AB. Limited financial interest from options in Sol Voltaics AB. M.T. Bjrk: Chief Technology Officer of Sol Voltaics AB. Limited financial interest from options in Sol Voltaics AB. L. Samuelson: Chief Scientific Officer of Sol Voltaics AB. Limited financial interest from options in Sol Voltaics AB. M.H. Magnusson: Limited financial interest from options in Sol Voltaics AB.

■ ACKNOWLEDGMENTS

This work was carried out at Sol Voltaics and within NanoLund and the MyFab cleanroom infrastructure. It was supported by the Knut and Alice Wallenberg foundation project "Aerotaxy: a revolutionary new way to grow semiconductor nanowires". Funding has also been received from the Swedish Energy Agency, and from the European Union's Horizon 2020 research and innovation programme under Grants 696519, 641023 (Nano-Tandem) and the Marie Sklodowska-Curie Grant

DOI: 10.1021/acs.nanolett.7b04609
Nano Lett. 2018, 18, 1088−1092

(656208). This article reflects only the authors' view and the Funding Agency is not responsible for any use that may be made of the information it contains.

REFERENCES

(1) Borgström, M. T.; Wallentin, J.; Heurlin, M.; Fält, S.; Wickert, P.; Leene, J.; Magnusson, M. H.; Deppert, K.; Samuelson, L. *IEEE J. Sel. Top. Quantum Electron.* **2011**, *17* (4), 1050−1061.
(2) Lapierre, R. R.; Chia, A. C. E.; Gibson, S. J.; Haapamaki, C. M.; Boulanger, J.; Yee, R.; Kuyanov, P.; Zhang, J.; Tajik, N.; Jewell, N.; Rahman, K. M. A. *Phys. Status Solidi RRL* **2013**, *7* (10), 815−830.
(3) Otnes, G.; Borgström, M. T. *Nano Today* **2017**, *12*, 31−45.
(4) Mann, S. A.; Oener, S. Z.; Cavalli, A.; Haverkort, J. E. M.; Bakkers, E. P. A. M.; Garnett, E. C. *Nat. Nanotechnol.* **2016**, *11* (12), 1071−1075.
(5) Cao, L.; Fan, P.; Vasudev, A. P.; White, J. S.; Yu, Z.; Cai, W.; Schuller, J. A.; Fan, S.; Brongersma, M. L. *Nano Lett.* **2010**, *10* (2), 439−445.
(6) Åberg, I.; Vescovi, G.; Asoli, D.; Naseem, U.; Gilboy, J. P.; Sundvall, C.; Dahlgren, A.; Svensson, K. E.; Anttu, N.; Björk, M. T.; Samuelson, L. *IEEE J. Photovoltaics* **2016**, *6* (1), 185−190.
(7) Wallentin, J.; Anttu, N.; Asoli, D.; Huffman, M.; Aberg, I.; Magnusson, M. H.; Siefer, G.; Fuss-Kailuweit, P.; Dimroth, F.; Witzigmann, B.; Xu, H. Q.; Samuelson, L.; Deppert, K.; Borgström, M. T. *Science* **2013**, *339* (6123), 1057−1060.
(8) Van Dam, D.; Van Hoof, N. J. J.; Cui, Y.; Van Veldhoven, P. J.; Bakkers, E. P. A. M.; Gómez Rivas, J.; Haverkort, J. E. M. *ACS Nano* **2016**, *10* (12), 11414−11419.
(9) Yao, M.; Huang, N.; Cong, S.; Chi, C. Y.; Seyedi, M. A.; Lin, Y. T.; Cao, Y.; Povinelli, M. L.; Dapkus, P. D.; Zhou, C. *Nano Lett.* **2014**, *14* (6), 3293−3303.
(10) Cui, Y.; Wang, J.; Plissard, S. R.; Cavalli, A.; Vu, T. T. T.; Van Veldhoven, R. P. J.; Gao, L.; Trainor, M.; Verheijen, M. A.; Haverkort, J. E. M.; Bakkers, E. P. A. M. *Nano Lett.* **2013**, *13* (9), 4113−4117.
(11) Yao, M.; Cong, S.; Arab, S.; Huang, N.; Povinelli, M. L.; Cronin, S. B.; Dapkus, P. D.; Zhou, C. *Nano Lett.* **2015**, *15* (11), 7217−7224.
(12) Nakai, E.; Chen, M.; Yoshimura, M.; Tomioka, K.; Fukui, T. *Jpn. J. Appl. Phys.* **2015**, *54* (1), 015201.
(13) Mariani, G.; Zhou, Z.; Scofield, A.; Huffaker, D. L. *Nano Lett.* **2013**, *13* (4), 1632−1637.
(14) Boulanger, J. P.; Chia, A. C. E.; Wood, B.; Yazdi, S.; Kasama, T.; Aagesen, M.; LaPierre, R. R. *IEEE J. Photovoltaics* **2016**, *6* (3), 661−667.
(15) Heurlin, M.; Magnusson, M. H.; Lindgren, D.; Ek, M.; Wallenberg, L. R.; Deppert, K.; Samuelson, L. *Nature* **2012**, *492* (7427), 90−94.
(16) Yang, F.; Messing, M. E.; Mergenthaler, K.; Ghasemi, M.; Johansson, J.; Wallenberg, L. R.; Pistol, M.-E.; Deppert, K.; Samuelson, L.; Magnusson, M. H. *J. Cryst. Growth* **2015**, *414*, 181−186.
(17) Metaferia, W.; Persson, A. R.; Mergenthaler, K.; Yang, F.; Zhang, W.; Yartsev, A.; Wallenberg, R.; Pistol, M. E.; Deppert, K.; Samuelson, L.; Magnusson, M. H. *Nano Lett.* **2016**, *16* (9), 5701−5707.
(18) Magnusson, M. H.; Ohlsson, B. J.; Björk, M. T.; Dick, K. A.; Borgström, M. T.; Deppert, K.; Samuelson, L. *Front. Phys.* **2014**, *9* (3), 398−418.
(19) Holm, J. V.; Jørgensen, H. I.; Krogstrup, P.; Nygard, J.; Liu, H.; Aagesen, M.; Nygård, J.; Liu, H.; Aagesen, M. *Nat. Commun.* **2013**, *4*, 1498.
(20) Demichel, O.; Heiss, M.; Bleuse, J.; Mariette, H.; Fontcuberta i Morral, I. A. *Appl. Phys. Lett.* **2010**, *97*, 201907.
(21) Gutsche, C.; Niepelt, R.; Gnauck, M.; Lysov, A.; Prost, W.; Ronning, C.; Tegude, F. J. *Nano Lett.* **2012**, *12* (3), 1453−1458.
(22) Cusano, D. A. *Solid State Commun.* **1964**, *2*, 353−358.

DOI: 10.1021/acs.nanolett.7b04609
Nano Lett. 2018, 18, 1088−1092